

# Morphology and melting behaviour of semi-crystalline poly(ethylene terephthalate):

## 3. Quantification of crystal perfection and crystallinity

F. Fontaine and J. Ledent

*Laboratory of Experimental Physics, Institute of Physics, University of Liège, Sart-Tilman, B-4000 Liège, Belgium*

and G. Groeninckx and H. Reynaers

*Department of Chemistry, Laboratory of Macromolecular and Organic Chemistry, University of Leuven, Celestijnenlaan 200 F, B-3030 Heverlee, Belgium*

(Received 9 February 1981)

The semi-crystalline state of bulk-crystallized poly(ethylene terephthalate) and its relation to the melting behaviour of the polymer have been thoroughly investigated as a function of the thermal history by wide-angle X-ray diffraction. The experimental data, analysed according to the method of Ruland, allow estimation of the absolute degree of crystallinity and the diffuse disorder scattering. The results of this study give a better and more complete insight into the complex thermal behaviour of PET, moreover they corroborate the need for a broad experimental approach in studies related to the melting behaviour of polymers.

**Keywords** Polymers; crystallinity; morphology; melting behaviour; crystallinity; poly(ethylene terephthalate)

### INTRODUCTION

In the past numerous studies have been devoted to the relation thermal history-morphology-melting behaviour of PET in the semi-crystalline state<sup>1-6</sup>.

These studies, mostly limited to observations by differential scanning calorimetry, have provided interesting and reliable information on the complex melting behaviour of PET. Although differential scanning calorimetry (d.s.c.) is a very sensitive tool in detecting morphological structure changes in semi-crystalline polymers, the results obtained by this technique alone do not inform on the exact morphology and the absolute value of the degree of crystallinity of the sample under investigation. An estimate of the degree of crystallinity by d.s.c., however, can be obtained if a reasonable value for  $\Delta H^\circ$ , the heat of fusion of an infinite crystal is available<sup>7</sup>. The information given by the degree of crystallinity is low and does not reflect the subtle morphological changes which are on the basis of the melting behaviour. A simple theoretical expression for the observed melting temperature of a chain-folded polymer crystal is given by the Thomson-Gibbs equation<sup>8</sup>:

$$T_m = T_m^\circ \left( 1 - \frac{2\sigma_e}{\Delta H^\circ l_c} \right) \quad (1)$$

where  $T_m^\circ$  is the melting temperature of an infinitely thick and perfect crystal,  $\sigma_e$  is the specific end-surface free energy of the crystals and  $l_c$  their thickness. It is clear that neither the shape of the melting endotherms nor their position on the temperature scale in a d.s.c.-trace inform on the crystal thickness distribution in the sample<sup>9</sup> or the

mean surface free energy which is related to order-disorder in the folded-chains at the interfaces of the crystals. The state of crystal perfection within the lamellae is also not accounted for.

Although the role of crystal perfection in thermal studies has been recognized<sup>2</sup>, there have been no reports on the quantification of this parameter with regard to thermal analysis.

Wide-angle X-ray diffraction, however, is directly related to order and disorder of matter, hence crystallinity. Within the frame of the two-phase concept for semi-crystalline polymers, different procedures have been described to derive the degree of crystallinity from the diffraction pattern<sup>10-17</sup>. In actual fact a further study of the crystallinity of PET is only justified as far as new information can be obtained for a better understanding of the relation between the polymer superstructure and its melting behaviour.

It is the aim of this paper to present data obtained by an absolute crystallinity method proposed by Ruland<sup>11</sup>. This method has a sound theoretical basis and, although time consuming in experimental approach and computation, gives at once an absolute degree of crystallinity and an isotropic disorder parameter reflecting the deviations of the atoms from their ideal positions in the crystalline phase.

The experiments described below on PET-samples, obtained by relatively simple as well as by complex thermal treatments, give evidence for crystal perfection phenomena in all cases. The relevance of this factor to the melting behaviour is discussed in relation with results obtained previously by other experimental approaches: density, SAXS and d.s.c.

## THEORY

The intensity of the X-rays scattered over all angles by an assemblage of atoms is independent of their state of order or disorder. If one can make a delimitation of the scattering due to the crystalline and amorphous parts of a semi-crystalline polymer sample, then the crystalline fraction of the specimen can be obtained by making the ratio of the integrated crystalline scattering to the total scattering. Ruland proposed the following equation:

$$x_c = \frac{\int_0^{\infty} s^2 I_c(s) ds}{\int_0^{\infty} s^2 I(s) ds} \cdot K \quad (2)$$

Here  $s$  stands for  $\frac{2}{\lambda} \sin \theta$ ,  $I(s)$  represents the coherent X-ray scattering and  $I_c(s)$  part of the intensity due to the crystalline material.

$K$  is given by:

$$K = \frac{\int_0^{\infty} s^2 \bar{f}^2 ds}{\int_0^{\infty} s^2 \bar{f}^2 D ds} \quad (3)$$

$\bar{f}^2$  stands for the weighted mean square atomic-scattering factor of the polymer and is given by

$$\frac{\sum N_i f_i^2}{\sum N_i}$$

where  $N_i$  is the number of atoms of type  $i$  and  $f_i$  is the atomic form factor of the  $i$ th atom.  $D$  is a Gaussian lattice imperfection factor and is assumed to be given by  $e^{-ks^2}$ ,  $k$  being the sum of three terms: thermal motions and lattice imperfections of the first and second kind. Equation (2) can be used in practice for specimens with random orientation of the crystallites, if crystalline peaks and background can be separated, and for a known imperfection factor  $k$ , using finite angular ranges for the integrals (minimum angle  $s_0$  – maximum angle  $s_p$ ). Here equation (2) is used in a slightly modified version suggested by Vonk<sup>17</sup>. Vonk started from Ruland's empirical finding<sup>11</sup> that  $K$  can be considered as a linear function of  $s_p^2$ :

$$K = 1 + b s_p^2 \quad (4)$$

where  $b$  is equal to  $k/2$  and  $s_p$  is the upper limit of integration. Writing

$$\frac{\int_0^{s_p} s^2 I(s) ds}{\int_0^{s_p} s^2 I_c(s) ds} = R(s_p)$$

and rearranging equation (2) after substitution of  $K$  by equation (4) one gets

$$R(s_p) \sim \frac{1}{x_c} + \frac{k}{2x_c} s_p^2 \quad (5)$$

In this equation, the symbol  $\sim$  stands for equality when  $s_p$  reaches infinity; for small values of  $s_p$ , however,  $R(s_p)$  plotted along a  $s_p^2$ -axis, actually oscillates around a straight line of equation

$$y(s_p) = \frac{1}{x_c} + \frac{k}{2x_c} s_p^2 \quad (6)$$

According to this relation the crystallinity of the sample and the imperfection factor are obtained from the intercept and the slope of a plot of  $y$  versus  $s_p^2$ .

For full details on the theory, the reader is referred to the original papers of Ruland<sup>11</sup>, Kavesh *et al.*<sup>14</sup> and Vonk<sup>17</sup>.

## EXPERIMENTAL

Amorphous PET sheets were kindly supplied by Agfa-Gevaert N.V., Antwerp. The intrinsic viscosity of the polymer in a phenol-*o*-dichloro-benzene mixture (60/40) at 25°C is 0.6, i.e.,  $\bar{M}_v$  is 37200 ( $\bar{M}_v$  is the viscosity-average molecular weight).

Isothermal crystallization of PET from the glassy state was carried out in a vacuum oven at various temperatures (100°C <  $T_c$  < 245°C). The crystallization time (17 h) was long enough to ensure complete crystallization.

Annealing treatments (see Tables 3 and 4) were performed on semicrystalline samples, isothermally crystallized from the glassy state at low  $T_c$  (100°C) and high  $T_c$  (200°C), respectively.

In order to avoid thermal lag effects upon annealing, samples of 2 mm thickness were used, the actual sample for the diffractometer (4 mm thickness) was obtained by superimposing two plates annealed at the same time under the same conditions.

The samples were analysed with respect to changes in crystallinity and crystal perfection by wide-angle X-ray diffraction. WAXD patterns were recorded in the reflection mode using a Philips vertical diffractometer equipped with a proportional counter and a pulse-height analyser. A copper target was used and monochromatization was simulated by using a pair of Ross balanced filters.

Ni and Co foils of approximate optimal thickness were obtained from Goodfellow Metals Ltd. (Cambridge) and a match on the white radiation background was realized by the inclination method<sup>18</sup>. Intensities were measured in the step-scanning mode.

Small steps ( $0.05^\circ 2\theta$ ) were used to scan sharp reflections, larger steps were allowed as a function of loss of detail in the spectrum at higher angles. The total pattern ( $8^\circ < 2\theta < 110^\circ$ ) was recorded generally in three parts which afterwards were merged to one master-spectrum by scaling of the intensities in overlapping regions.

Other special precautions due to the low X-ray absorption coefficient of PET were considered according to Milberg<sup>19</sup> and Vonk<sup>20</sup>: a sample thickness of 4 mm, scatter slits always larger than the divergence slits,

sample mounting in the diffractometer in such a way that no interaction of scattered radiation with the sample holder was possible.

Typical diffractometer runs involve data collection at about 550 angular positions spread for instance over the following angular range:  $8^\circ$ – $50^\circ$   $2\theta$ ,  $34^\circ$ – $86^\circ$   $2\theta$ ,  $80^\circ$ – $110^\circ$   $2\theta$ . The raw data were treated by the computer program FFCRYST<sup>17</sup>. This program removes spurious intensities, applies the polarization correction, scales and merges the data of the different angular ranges to one master set. The critical step in Ruland's X-ray crystallinity determination is the separation of the crystalline peaks from the background of the amorphous scattering. In this work fitting of the scattering curve of a completely amorphous sample to the observed intensities for a semicrystalline specimen is done according to Vonk<sup>17</sup>; it is judged from the inspection of the diffractometer tracings that in the intervals  $8^\circ$ – $12.9^\circ$   $2\theta$ ,  $19.3^\circ$ – $20.3^\circ$   $2\theta$ ,  $29.4^\circ$ – $31.7^\circ$   $2\theta$ ,  $34.5^\circ$ – $39.2^\circ$   $2\theta$ ,  $44.6^\circ$ – $45.5^\circ$   $2\theta$ ,  $56.4^\circ$ – $64.2^\circ$   $2\theta$ ,  $68.5^\circ$ – $78.8^\circ$   $2\theta$ ,  $87.0^\circ$ – $94.3^\circ$   $2\theta$ , crystalline peaks are entirely absent (see Figure 1). It is well known from other work in the field, however, that for the case of PET there is always an uncertainty in the separation of the crystalline peaks from the background of amorphous and incoherent scattering<sup>16,17,27</sup>; this introduces a systematic error but the trend of the results will not be affected as long as the separation of both components is always done in the same way.

The observed intensities are brought on absolute scale by multiplying with a scale factor  $T(s_p)$  obtained from equation (6) in the angular range  $s=0.8$  to  $s=1.1$ .

$$T(s_p) = \frac{\int_0^{s_p} (\bar{f}^2 + \bar{J}) s^2 ds}{\int_0^{s_p} I_{\text{tot}} s^2 ds} \quad (6)$$

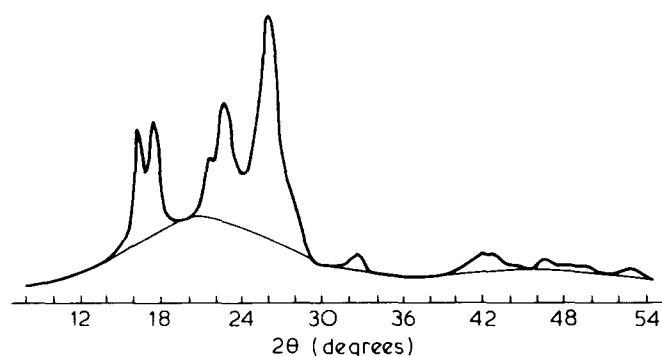


Figure 1 Separation of the crystalline peaks from the continuous background in the X-ray diagram

Here  $I_{\text{tot}} = I + I_{\text{inc}}$  and  $\bar{J}$  is the average of the incoherent intensities in electron units, for the atoms present. Finally this curve is reduced to coherent intensities by subtraction of  $\bar{J}$ .

## RESULTS AND DISCUSSIONS

### Isothermally crystallized PET-samples

The results of crystallinity measurements obtained by Ruland's method are presented in Table 1. Typical plots of  $R(s_p)$  as a function of  $s_p^2$  are shown in Figure 2. Function  $y(s_p)$  is obtained by linear least-square fitting of the data; this procedure, however, is hampered by the considerable oscillations of the  $R(s_p)$  values at the lowest  $s_p^2$  values.

In order to assess the influence of this factor on the final result, the fitting is executed eight times for different lower limits of  $s_p^2$  and the same upper limit. Results are shown in Table 2 for a sample crystallized at  $T_c = 200^\circ\text{C}$ . The mean value of  $x_c$  and  $k$  is calculated from all non-bracketed values.

The results in Table 1 are essentially a quantification of the existing knowledge: it is clear from earlier work<sup>21</sup> that there are large changes of the state of order of the

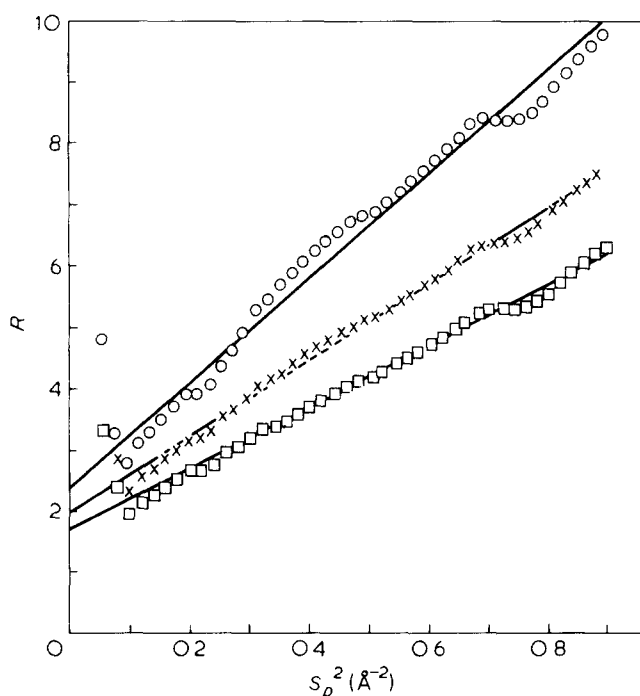


Figure 2 Plot of  $R$  versus  $s_p^2$  for isothermally crystallized PET samples. ( $T_c = 150^\circ\text{C}$ :  $\circ$ ;  $T_c = 200^\circ\text{C}$ :  $\times$ ;  $T_c = 245^\circ\text{C}$ :  $\square$ )

Table 1 Morphological parameters and melting temperatures of PET samples isothermally crystallized at different temperatures

Sample	Crystallization temperature ( $^\circ\text{C}$ )	Degree of crystallinity $X_d^a$	Degree of crystallinity $X_{d.s.c.}^b$	Degree of crystallinity $X_{WAXS}^c$	Disorder parameter $k^c$	Average melting temperature $T_m^{av}$ ( $^\circ\text{C}$ )
1	150	39	33	43	7.3	— <sup>e</sup>
2	200	54	41	53	6.7	240 <sup>d</sup>
3	245	61	45	61	6.3	266 <sup>d</sup>

<sup>a</sup> Calculated from density increase. See ref (21)

<sup>b</sup> Calculated from d.s.c. data  $-\Delta H^0 = 28.1$  cal/g. See ref (21)

<sup>c</sup> Obtained by Ruland's method

<sup>d</sup> See ref (21)

<sup>e</sup> Transforms at a scanning rate of  $8^\circ\text{C min}^{-1}$  in d.s.c.

crystalline regions as a function of the isothermal crystallization temperature and in the degree of crystallinity as well. The significance of the present data is rather in the fact that they add new information to the existing data. In the past, density measurements and d.s.c. data have been used extensively to monitor changes in crystallinity and crystal perfection<sup>21-24</sup>. Density, however, is not directly sensitive to crystallinity but if the density of a 100% crystalline specimen ( $\rho_c$ ) and that of a completely amorphous specimen  $\rho_a$  are known, then an apparent degree of crystallinity expressed as a volume fraction can be calculated for a semi-crystalline sample with density  $\rho$  using the relation<sup>25</sup>:

$$X_d = \frac{\rho - \rho_a}{\rho_c - \rho_a} \quad (7)$$

The difficulties inherent to this method have been discussed recently in great detail by Fisher and Fakirov<sup>23</sup>.

The d.s.c. method is based on a thermodynamic definition of order and it requires knowledge of the heat of fusion of a fully crystalline polymer:  $\Delta H^\circ$ .  $X_{d.s.c.}$ , expressed as a weight function, can be determined according to:

$$X_{d.s.c.} = \frac{\Delta H^{exp}}{\Delta H^\circ} \quad (8)$$

Table 2 Results of crystallinity determination for different lower limits in  $s_p^2$  ( $T_c = 200^\circ\text{C}$ )

Lower limit	Crystallinity ( $X_{WAXD}$ )	k-factor
0.06	(41)	(4.4)
0.08	(52)	(6.5)
0.10	(55)	(7.2)
0.12	54	7.0
0.14	53	6.8
0.16	53	6.7
0.18	52	6.6
0.20	51	6.4
	$X_{WAXD} = 53$	$k = 6.7$

where  $\Delta H^{exp}$  represents the measured heat of fusion of a semi-crystalline sample.

There is poor agreement between crystallinity data obtained by both methods in the case of PET<sup>23</sup> and although Fakirov *et al.*<sup>26</sup> consider  $X_{d.s.c.}$  as the most relevant quantity for describing the amount of crystalline material in a sample, there is need for an independent control of this statement. This point will be further clarified by the study of the annealed samples.

With regard to our previous work<sup>21</sup> the results of Table 1 provides two new parameters: an absolute degree of crystallinity and a disorder parameter. Both are obtained by WAXD, a technique directly sensitive to the amounts of crystalline and amorphous scattering masses and the crystal perfection. Both parameters are in agreement with the general trend of morphological parameters as a function of crystallization temperature: the increase in crystallinity was already observed by density and d.s.c.; the value of  $k$  decreases as a function of increasing crystallization temperature reflecting the formation of more perfect crystals with enhanced thermal stability, as observed by d.s.c.

#### Annealed PET samples

Annealing above a high crystallization temperature ( $T_c = 200^\circ\text{C}$ ). In order to study the structural changes occurring upon annealing, PET samples isothermally crystallized at high  $T_c$  ( $T_c = 200^\circ\text{C}$ ), were slowly heated to higher annealing temperatures  $T_{an}$  ( $200^\circ\text{C} < T_{an} < 250^\circ\text{C}$ ). The complete annealing procedure is given in Table 3. After slow cooling to room temperature the samples were analysed with respect to the long spacing (SAXS), degree of crystallinity (density, d.s.c., WAXD) order-disorder (WAXD) and melting temperature (d.s.c.).

The  $R$  versus  $s_p^2$  plots for samples 1, 2 and 5 in Table 3 are represented in Figure 3; sample 3 and sample 4 are omitted for clarity. It has been reported recently<sup>21</sup> that samples crystallized at high  $T_c$  ( $T_c \geq 200^\circ\text{C}$ ) exhibit a very well-developed lamellar morphology within the spherulites and as a consequence can be analysed within the frame of the two-phase concept. The annealing

Table 3 Morphological parameters and melting temperatures of PET, crystallized at  $T_c = 200^\circ\text{C}$  and annealed at different temperatures (slow heating)

Sample	Thermal history	Mean long spacing $L$ (Å)	Degree of crystallinity $X_d^a$ (%)	Degree of crystallinity $X_{d.s.c.}^b$ (%)	Degree of crystallinity $X_{WAXD}^c$ (%)	Disorder parameter $k^c$	Average melting temperature $T_m^{av}$ ( $^\circ\text{C}$ )
1	$T_c = 200^\circ\text{C}$	126	54	41	53	6.7	240
2	As for sample 1 +(200°–215° C; 4° C/h) +(215° C for 17 h)	125	55	47	60	6.3	243
3	As for sample 2 +(215°–230° C; 4° C/h) +(230° C for 17 h)	125	58	49	59	5.7	248
4	As for sample 3 +(230°–245° C; 2° C/h) +(245° C for 17 h)	128	59	48	58	5.7	252
5	As for sample 4 +(245°–250° C; 2° C/h) +(250° C for 17 h)	129	61	50	63	5.4	256

<sup>a</sup> Calculated from density measurements see ref (21)

<sup>b</sup> Calculated from d.s.c. data  $-\Delta H^0 = 28.1$  cal/g see ref (21)

<sup>c</sup> Obtained by Ruland's method

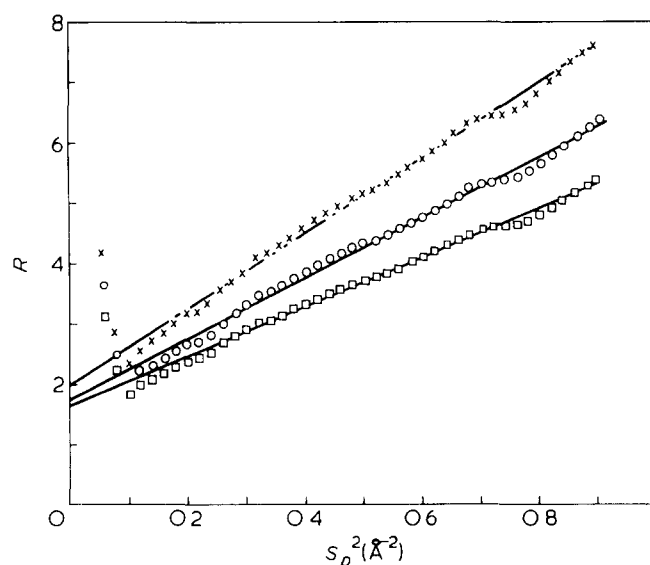


Figure 3 Plot of  $R$  versus  $s_{\rho}^2$  for PET samples annealed above a high crystallization temperature ( $T_c = 200^{\circ}\text{C}$ ). ( $T_{an} = 200^{\circ}\text{C}$ :  $\square$ ;  $T_{an} = 215^{\circ}\text{C}$ :  $\circ$ ;  $T_{an} = 250^{\circ}\text{C}$ :  $\times$ )

treatments reported in Table 3 involve an increase in the average melting temperature without any change in the long spacing of the super-structure. The variations in degree of crystallinity obtained by d.s.c. and WAXD—although different in numerical value—evolute in the same direction; moreover an important increase in crystallinity is observed by both methods for the first heating stage up to  $T_{an} = 215^{\circ}\text{C}$ . Apparently, the density method does not reflect this increase. The disorder parameter ' $k$ ' exhibits a decrease with increasing annealing temperature, the other parameters remaining approximately constant above  $T_{an} = 215^{\circ}\text{C}$ .

These data allow us to construct the following picture of the molecular rearrangements in the existing superstructure as a result of the annealing treatments considered. The complete absence of any change in long spacing strongly indicates that no large scale melting phenomena occurred. The increase in degree of crystallinity by heating from  $200^{\circ}\text{C}$  up to  $215^{\circ}\text{C}$  reveals a crystal thickening process without change in long spacing probably due to crystal perfection phenomena at the boundary layers of the crystalline and amorphous phases. For  $T_{an} > 215^{\circ}\text{C}$ , only a decrease in the disorder parameter is observed; hence the further melting temperature increase has to be ascribed to an overall increase in crystalline perfection. More evidence for this crystal perfection, especially at the crystalline-amorphous boundaries, comes from our SAXS experiments<sup>22</sup>: a small but systematic increase in total scattered radiation at small angles was observed as a function of increasing  $T_{an}$ . This effect is directly related to  $\Delta\rho$ , the difference in electron density between the amorphous and crystalline layers: annealing removes the structural distortions and leaves a better delimitation at the level of the amorphous-crystalline interface and therefore a greater  $\Delta\rho$  value. A similar observation has been reported by Scotton *et al.*<sup>27</sup>. A pictorial representation of the effect of annealing on the morphology at the crystalline-amorphous boundary layer is given in Figure 4. Additional evidence for these boundary layer effects can be obtained from a detailed analysis of the intensity in the tail of the small-angle scattering pattern<sup>28</sup> or by way of the correlation

function<sup>29</sup> and this route will be further exploited. The present findings are extremely important with regard to the relation morphology–melting behaviour of semicrystalline polymers. With respect to the results of Table 3 it can be stated that 'in the case of PET' crystal perfection always occurs upon annealing and that the effect of lattice imperfections on the melting behaviour is not negligible.

It has to be noted for annealing temperatures  $T_{an} > 215^{\circ}\text{C}$ , that the melting temperature increase has to be attributed to crystal perfection alone and not to crystal thickening, as often suggested in studies restricted to differential scanning calorimetry alone.

The peculiarity of PET with respect to crystal perfection is also well-documented by evidence from crystal structure studies, the cell parameters being dependent on the annealing conditions<sup>30,31</sup>.

The role of crystal perfection and its implications on the melting behaviour of PET was already recognized by Holdsworth and Tuner-Jones<sup>2</sup> although these authors did not present directly quantitative evidence. It should be noted that all the samples mentioned in Table 3, when scanned in the d.s.c. at  $4^{\circ}\text{C min}^{-1}$ , exhibit a complex melting behaviour: two endotherms are observed<sup>22</sup>. Endotherm I (lowest melting peak) corresponds to the melting of the crystalline structure as obtained by annealing and endotherm II (highest melting peak) reflects the melting of a fraction of the original structure which has undergone transformations (here only crystal perfection) resulting in enhanced thermal stability.

Annealing above a low crystallization temperature ( $T_c = 100^{\circ}\text{C}$ ). It has already been shown<sup>22</sup> that the semicrystalline state of PET, crystallized at  $T_c = 100^{\circ}\text{C}$ , is ill-defined—in the sense of the absence of a stacked lamellar morphology—and as a consequence is highly susceptible to transformations upon annealing at higher temperatures. It appears indeed impossible to determine the average melting temperature of such a sample by d.s.c. due to the very fast transformation processes occurring

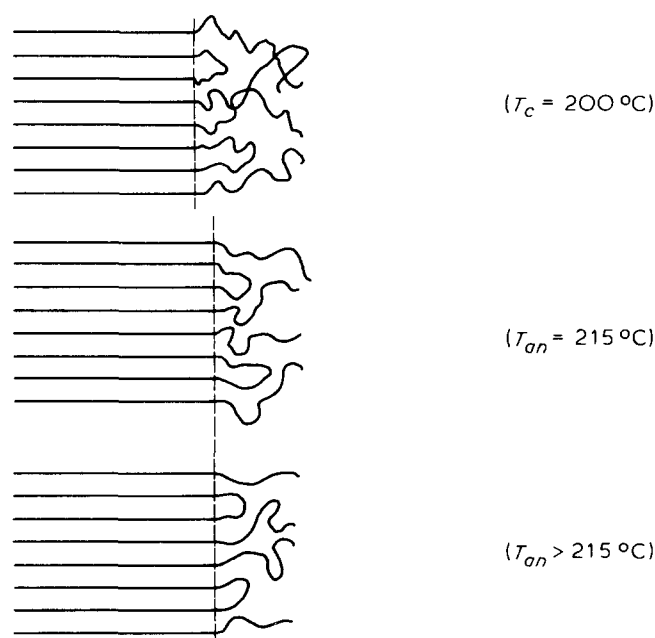


Figure 4 Ordering and smoothing effect at the crystalline–amorphous interface of the lamellae

Table 4 Morphological parameters of PET samples with different annealing histories

Sample*	Thermal history	Mean long spacing $L$ (Å)	Degree of crystallinity $X_d^a$ (%)	Degree of crystallinity $X_{d.s.c.}^b$ (%)	Degree of crystallinity $X_{WAXD}^c$ (%)	Disorder parameter $k^c$	Average melting temperature $T_m^{av}$ (°C)
(1)	$T_c = 100^\circ\text{C}$ for 17 h	95	29	27	—	—	—
2	As for sample 1 +(100°–245° C-slow heating) +(245° C for 17 h)	126	60	49	63	5.9	252 <sup>d</sup>
3	As for sample 1 +(100°–245° C: quickly) +(245° C for 17 h)	152	60	47	59	5.3	262 <sup>d</sup>
(4)	$T_c = 245^\circ\text{C}$ for 17 h	171	60	45	61	6.3	266
(5)	$T_c = 200^\circ\text{C}$ for 17 h +(200°–245° C—see sample 4 of Table 3)	128	59	48	58	5.7	252

\* Samples between brackets are entered for reference

<sup>a</sup> Calculated from density measurements. See ref (21)

<sup>b</sup> Calculated from d.s.c.—data  $-\Delta H^0 = 28.1$  cal/g. See ref (21)

<sup>c</sup> Obtained by Ruland's method

<sup>d</sup> Obtained from ref (22)

even at high d.s.c. heating rates. The wide-angle diffraction pattern of this sample fails to show single well-resolved reflections and this bears out the possibility of determining a degree of crystallinity and a disorder parameter by Ruland's method. The figures for  $X_d$  and  $X_{d.s.c.}$  in Table 4 (sample 1) should also be considered as rough approximations. Two samples crystallized at  $T_c = 100^\circ\text{C}$  for 17 h were subjected to different annealing treatments but finally kept for 17 h at  $T_{an} = 245^\circ\text{C}$ . The first sample was heated very slowly up to  $T_{an} = 245^\circ\text{C}$  and kept for 17 h at this temperature, the second one was heated very quickly to  $T_{an} = 245^\circ\text{C}$  and stayed at this temperature for a further 17 h. Both samples were then slowly cooled to room temperature and analysed with respect to their morphology. It is clear that quick heating (sample 3, Table 4) to  $T_{an} = 245^\circ\text{C}$  implies partial melting of the original structure followed by immediate recrystallization in more stable and thus higher melting species<sup>22</sup>. It is assumed that the newly formed crystallites melt again and recrystallize several times until the annealing temperature is reached. The absence of 'complete' melting during this heating procedure is supported by the fact that the mean long spacing and the final melting temperature of the annealed sample are lower than those for a sample crystallized under isothermal conditions at  $T_c = 245^\circ\text{C}$ . There is, however, a large increase in degree of crystallinity and the disorder parameter of the sample is low with  $k = 5.3$ . Compare for example with  $k = 7.3$  for the sample isothermally crystallized at  $150^\circ\text{C}$ . We now compare sample (3) with sample (2). For sample (2), the annealing temperature  $T_{an} = 245^\circ\text{C}$  was reached slowly at a heating rate of  $4^\circ\text{C/h}$ ; its final degree of crystallinity is higher than for sample (3), where part of the material did not recrystallize, possibly due to the rejection of low molecular weight material, and so does the disorder parameter which is equal to 5.9 as compared to  $k = 5.3$  for sample (3). Hence, in spite of the same annealing temperature  $T_{an} = 245^\circ\text{C}$  for both samples, sample (3) shows the largest increase in crystal perfection; this fact is of course entirely due to the melting processes occurring upon heating.

It has to be noted again that the density method is less suitable with regard to the detection of changes in crystallinity, whereas  $X_{d.s.c.}$  and  $X_{WAXD}$  exhibit the same trend. The change in long spacing of sample (2) is not as pronounced as for sample (3).

The total set of experiments reported in Table 4 forces us to conclude that for both annealing treatments—slow and quick heating of a sample isothermally crystallized at  $100^\circ\text{C}$ —annealing results in crystal thickening and crystal perfection. It remains however impossible—in contrast with the results of Table 3—to evaluate quantitatively the respective contributions of both parameters to the melting temperature increase: inspection of the degree of crystallinity obtained by density for the samples (2), (3), (4) and (5)—all with quite different thermal histories—clearly demonstrate the pitfalls of the density method with respect to changes in crystallinity.

## CONCLUSIONS

The complex melting behaviour of PET, as reflected by a second melting endotherm (the higher melting species) in a d.s.c.-trace, is intimately related to morphological changes in the microstructure of the semicrystalline sample during the scan.

Differential scanning calorimetry appears to be a very fast and extremely sensitive tool to detect even minor structural changes; this method, however, fails to give any direct information on the nature of the morphological changes involved and as a consequence must be always sustained by other experimental tools.

WAXD is directly sensitive to order and disorder on the molecular level in crystalline materials. If the diffraction data are obtained under suitable experimental conditions of monochromatization and counting technique then the degree of crystallinity, obtained by applying Ruland's analysis to the data, exhibits the same trend as the d.s.c. crystallinity; hence both methods appear to detect the same structural changes. Another result of Ruland's analysis is an estimate of the crystal perfection by means

of the disorder parameter  $k$ . Crystal perfection improves as a function of increasing isothermal crystallization temperature and for all annealing treatments on isothermally crystallized samples. Under favourable conditions (see the results of *Table 3*) crystal perfection is the unique factor involved for explaining the increase in the melting temperature of the sample. In all other cases reported, crystal thickness and crystal perfection change simultaneously and it is impossible to evaluate the exact respective contributions of both factors on the melting temperature increase.

It is clear from our experiments that the understanding of the morphological aspects of annealing in semi-crystalline PET and other polymers is only possible within a broad experimental approach of the problem.

#### ACKNOWLEDGEMENTS

The authors wish to thank IWONL/Agfa-Gevaert and the NFWO for equipment and financial support; they are also indebted to the computing centre of the University of Liège.

#### REFERENCES

- 1 Roberts, R. C. *Polymer* 1969, **10**, 117
- 2 Holdsworth, P. J. and Turner-Jones, A. *Polymer* 1970, **12**, 195
- 3 Bell, J. P. and Murayama, T. *J. Polym. Sci.* 1969, **1** 2, 1059
- 4 Roberts, R. C. *J. Polym. Sci. B* 1970, **8**, 381
- 5 Sweet, G. E. and Bell, J. P. *J. Polym. Sci. A-2* 1972, **10**, 1273
- 6 Nealy, D. L., Davis, T. G. and Kibler, C. J. *J. Polym. Sci. A-2* 1970, **8**, 2141
- 7 Metha, A., Gaur, U. and Wunderlich, B. *J. Polym. Sci., Polym. Phys. Edn.* 1978, **16**, 289
- 8 Hoffman, J. F. *SPE Trans.* 1964, **4** (4), 1
- 9 Haase, J., Hosemann, R. and Köhler, S. *Polymer* 1978, **19**, 1358
- 10 Johnson, J. E. *J. Appl. Polym. Sci.* 1959, **19**, 1358
- 11 Ruland, W. *Acta Crystallogr.* 1961, **14**, 1180
- 12 Bosley, D. E. *J. Appl. Polym. Sci.* 1964, **8**, 1521
- 13 Dumbleton, J. H. and Bowles, B. B. *J. Polym. Sci. A-2* 1966, **4**, 1951
- 14 Kavesh, S. and Schultz, J. M. *J. Polym. Sci. A-2* 1970, **8**, 243
- 15 Lindner, W. L. *Polymer* 1973, **14**, 9
- 16 Chung, F. H. and Scott, R. W. *J. Appl. Crystallogr.* 1973, **6**, 225
- 17 Vonk, C. G. *J. Appl. Crystallogr.* 1973, **6**, 148
- 18 Smelser, S. C., Henninger, E. H., Pings, C. J. and Wignall, G. D. *J. Appl. Crystallogr.* 1975, **8**, 8
- 19 Milberg, M. E. *J. Appl. Phys.* 1958, **29**, 64
- 20 Vonk, C. G. *Norelco Rep.* 1961, **8**, 92
- 21 Groeninckx, G., Reynaers, H., Berghmans, H. and Smets, G. *J. Polym. Sci., Polym. Phys. Edn.* 1980, **8**, 1311
- 22 Groeninckx, G. and Reynaers, H. *J. Polym. Sci., Polym. Phys. Edn.* 1980, **18**, 1325
- 23 Fisher, E. W. and Fakirov, S. *J. Mater. Sci.* 1976, **11**, 1041
- 24 Alfonso, C. G., Pedemonte, E. and Ponzetti, L. *Polymer* 1979, **20**, 104
- 25 Alexander, L. E. 'X-ray Diffraction Methods in Polymer Science', 1 Edn, New York, London, Sydney, Toronto, 1969, p 189
- 26 Fakirov, S., Fisher, E. W., Hoffman, R. and Schmidt, G. F. *Polymer* 1977, **18**, 1121
- 27 Sotton, M., Arnaud, A. M. and Rabourdin, C. *J. Appl. Polym. Sci.* 1978, **22**, 2585
- 28 Ruland, W. *J. Appl. Crystallogr.* 1971, **4**, 70
- 29 Vonk, C. G. *J. Appl. Crystallogr.* 1973, **6**, 81
- 30 Fakirov, S., Fisher, E. W. and Schmidt, G. F. *Makromol. Chem.* 1975, **176**, 2459
- 31 Kinoshita, Y., Nakamina, R., Kitano, Y. and Ashida, T. Joint ACS/JCS Honolulu meeting, *Polym. Prepr.* 1979, **20**(1), 454